Journal of Alloys and Compounds 504S (2010) S476–S479

Contents lists available at ScienceDirect

Journal of Alloys and Compounds

journal homepage: www.elsevier.com/locate/jallcom

Microstructure and mechanical properties of rapidly quenched Fe–6.5 wt.% Si alloy

Y.F. Liang, J.P. Lin, F. Ye*, Y.J. Li, Y.L. Wang, G.L. Chen

State Key Laboratory for Advanced Metals and Materials, University of Science and Technology Beijing, 30 Xueyuan Road, 100083 Beijing, PR China

ARTICLE INFO

Article history:
Received 5 July 2009
Received in revised form 3 March 2010
Accepted 7 March 2010
Available online 12 March 2010

Keywords:
Fe–6.5 wt.% Si
Rapid quenching
Microstructure
Mechanical properties
Ductility

ABSTRACT

Suction cast technique is employed for producing Fe–6.5 wt.% Si alloy, which is very brittle at room temperature due to the appearance of ordered phases. The master alloy was melted and then rapidly quenched into a set of copper molds to form rod or sheet. Microstructure, micro-hardness and X-ray diffraction analyses were carried out to investigate its unique properties in comparison with conventionally cast method. The rapidly quenched sheets were cold rolled to investigate the quenching effect on its rolling workability. Rapid quenching combined with cold rolling with a large reduction ratio is effective to produce cold rolled Fe–6.5 wt.% Si alloy sheet.

1. Introduction

Fe–6.5 wt.% Si alloy has excellent soft magnetic properties compared with conventional silicon steel (with Si content ≤3.5 wt.%) [1]. As to its high Si content, Fe–6.5 wt.% Si alloy is very brittle at room temperature due to appearances of ordered phases like *B*2 and $D0_3$ [2,3]. The ductility of as cast Fe–6.5 wt.% Si alloy at room temperature is almost zero, thus hindering the production of this alloy by hot and cold rolling method [4].

There are several methods developed to avoid the brittle condition of this alloy at room temperature, such as Chemical Vapor Deposition (CVD) [5], Spray Forming [4,6], Direct Powder Rolling (DPR) [7], Dipping and Diffusion Annealing [8], Rapid Quenching [9,10]. Watanabe et al. reported that there was high ductility for rapidly solidified ribbons after fully annealing [11]. Nakamura et al. reported that quick quenching from 1100 °C suppressed the formation of *B*2 superlattice [12]. However, most of the rapidly quenched samples were thin foils with thickness of 30–50 μm or fibers with diameter of about 90 μm [13]. Meanwhile Kim et al. found that boron has the availability for Fe–6.5 wt.% Si alloy grain refinement [14].

In this paper, we studied microstructure, mechanical properties and rolling workability of rapidly quenched rods and sheets of Fe–6.5 wt.% Si alloy. It was found that decreasing the long-range order (LRO) parameter by enhancement of cooling rate is helpful for improving the working ductility.

2. Experimental methods

The master alloy was produced by melting industrial pure iron (99.5 wt.% Fe purity), boron iron (20.4 wt.% B, 0.05 wt.% C, Fe bal.), and metallic silicon (99 wt.% Si purity). The content of the elements in the alloy is listed in Table 1.

The master alloy was suction cast into a set of copper molds to form rods with different diameter or sheet with a thickness of 3 mm. The suction cast samples were spark cut to 2 mm thick and 15 mm wide and then cold rolled using a 4-high mill with working roll of 120 mm in diameter and rolling speed of 12 rpm. The reduction was 25%, 35% and 44% per pass for different sheets.

Optical microscopy was utilized to observe the microstructure evolution of the different quenched samples. The samples were etched with an 8% solution of nitric acid in pure water. Micro-Hardness Indenter MH-6 was used to measure hardness with a load of 100 g for 10 s, and Philips APD-10 X-ray diffractometer using Mo Kα radiation was applied to identify the structure.

3. Results and discussion

3.1. Microstructure

Fig. 1(a–d) shows the microstructure of conventionally cast sample and rapidly quenched samples. The average grain size was measured to be of 315, 92, and 63 μm for conventionally cast sample, Φ10 mm suction rod and 3 mm thick suction sheet, respectively. There were small sized and obvious dendrites in Φ1 mm suction rod. The grain boundaries were not smooth and the dendrite arm spacing was around 5 μm, which could be favorable to minimize the solidification segregation just like in spray formed powders [4]. It is observed that the grain size gets smaller when the

* Corresponding author. Tel.: +86 10 6233 3899.
E-mail address: yefeng@skl.ustb.edu.cn (F. Ye).

0925-8388/$ – see front matter © 2010 Elsevier B.V. All rights reserved.
doi:10.1016/j.jallcom.2010.03.075

Table 1
Chemical composition of Fe–6.5 wt.% Si (wt.%).

Si	B	C	Mn	S	P	O	Al	Fe
6.53	0.066	0.012	0.024	0.003	0.0098	0.0032	0.0059	Bal.

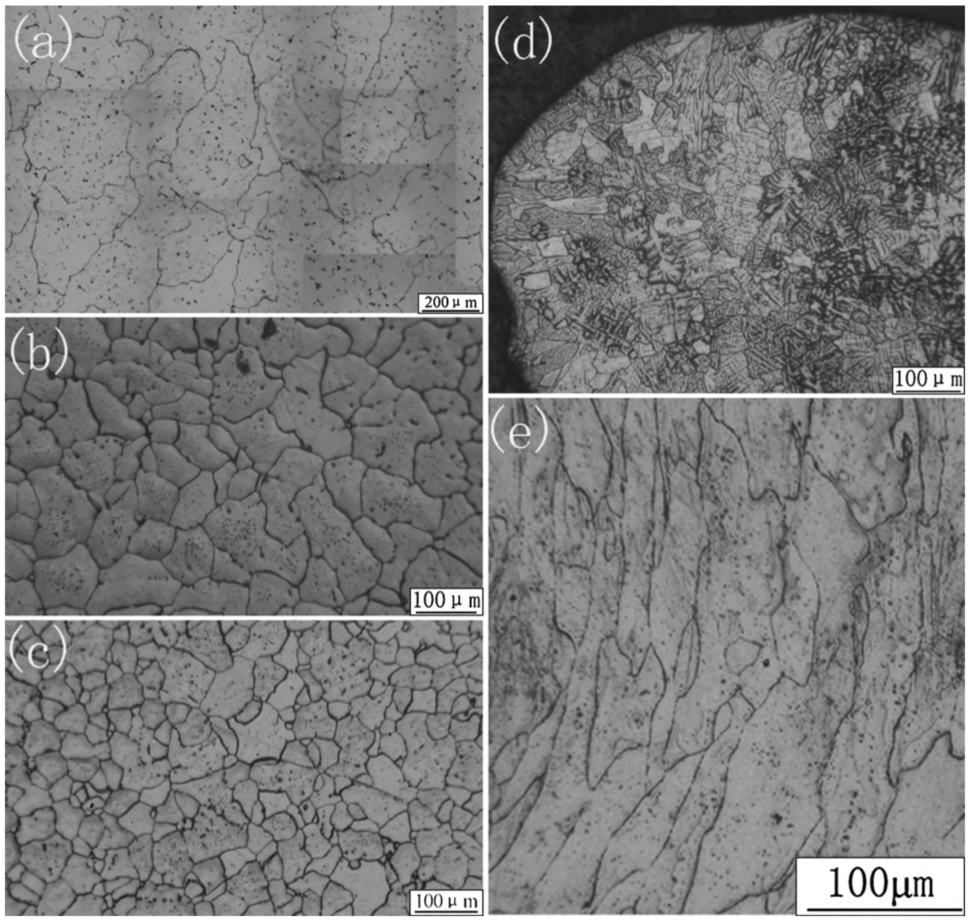

Fig. 1. Microstructure of Fe–6.5 wt.% Si alloy: (a) conventionally cast, (b) Φ10 mm suction cast, (c) 3 mm thick sheet suction cast, (d) Φ1 mm suction cast and (e) 3 mm sheet suction cast after cold rolling at reduction of 44%.

rod diameter decreases. For the 3 mm thick sheet, the grain size is smaller than Φ10 mm rod, but larger than Φ1 mm rod. After one pass of cold rolling at reduction of 44%, the grains of suction cast sheet were elongated to the rolling direction as shown in Fig. 1(e), where the shape factor of the elongated grains was found to be 5:1.

3.2. Mechanical properties

Fig. 2 shows the micro-hardness of Fe–6.5 wt.% Si alloy processed by various methods corresponding to Fig. 1. Micro-hardness for conventionally cast sample was larger than rapidly quenched ones either in rod or in sheet and it increased significantly after cold rolling for suction cast sheet.

Shin et al. [15] reported that the relation between micro-hardness and Si content can be expressed in the higher Si range as Eq. (1):

$$HV = -112 + 41.4 \text{ at.\% Si} \quad (1)$$

This equation was applicable at higher Si content of 7–13 at.% where micro-hardness was proportional to at.% of Si due to short-range ordering [16]. The micro-hardness of conventionally cast Fe–6.5 wt.% Si alloy was 387 ± 13 HV (Fig. 2), which agreed very well with Eq. (1) (Si content was 12.15 at.%, and calculated HV was 391). For rapidly quenched Fe–6.5 wt.% Si alloy with smaller grain size, the hardness decreased from 387 ± 13 to 358 ± 16 HV. This phenomenon contradicted with the Hall–Petch relationship.

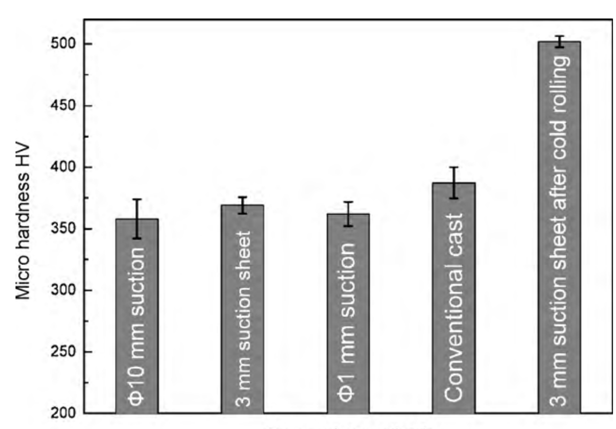

Fig. 2. Micro-hardness of Fe–6.5 wt.% Si alloy processed by various methods.

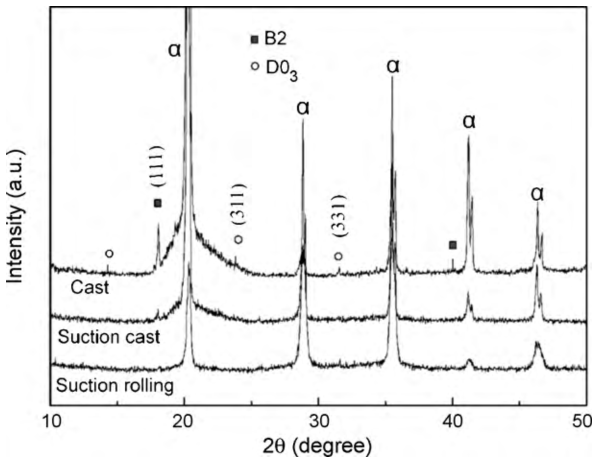

Fig. 3. X-ray diffraction spectra of Fe–6.5 wt.% Si alloy for: (a) conventionally cast, (b) 3 mm thick sheet suction cast and (c) 3 mm thick sheet suction cast after cold rolling.

The structure of conventionally cast and rapidly quenched samples was investigated by X-ray diffraction as shown in Fig. 3. One can find $B2$ and $D0_3$ phases in the conventionally cast sample. Intensities of ordered phases became lower for suction cast sample and became obscure for suction cast sheet after cold rolling.

Mixture of $B2$ and $D0_3$ phases would be responsible for the enhancement of micro-hardness in conventionally cast sample as revealed by Wittig and Frommeyer [17]. After rapid quenching, $B2$ ordered phases were observed while $D0_3$ phases were removed. $B2$ ordered phases were dissolved at high temperature, and then rapidly re-formed during cooling due to its continuous transformation. Rapid quenching cannot effectively suppress the continuous ordering reaction leading to the $B2$ structure. But it can suppress the first order of $B2$ to $D0_3$ reaction. Meanwhile the continuous transformation was known to be sensitive to the Si content [18]. For the rapidly quenched sample, e.g. in Fig. 1(d), the very fine microstructure and small segregation could be favorable to minimize the formation of the ordered phases.

The above results indicate that the softening by rapid quenching can be attributed to the disorder–order transition during the solidification. The LRO parameter could be determined by [19]

$$\mathrm{LRO} = \left[\frac{I^s/I_0^s}{I^f/I_0^f}\right]^{1/2} \tag{2}$$

where I^s and I^f are the intensities for the superlattice and fundamental lines for specific samples obtained by different ways, I_0^s and I_0^f are the intensities for the same lines in a fully ordered sample as indicated by PDF card #65-1835. The LRO parameters for the samples produced by different processing methods were calculated and given in Table 2. The LRO parameter of suction cast sheet was much smaller compared with conventionally cast one, and was even smaller after cold rolling.

In general, plastic deformation of ordered alloys can reduce the degree of LRO [20]. The LRO parameter decreases with the normal and shear strain, because the migration of uncoupled single dislocations destroys order [21]. For Fe–6.5 wt.% Si alloy sheet after cold rolling, the ordered phases became obscure and the degree of order was decreased.

Table 2
The long-range order (LRO) parameter of Fe–6.5 wt.% Si alloy for different processing methods.

Samples	LRO parameter
Conventionally cast	0.41
Suction cast	0.25
Suction cold rolling	0.10

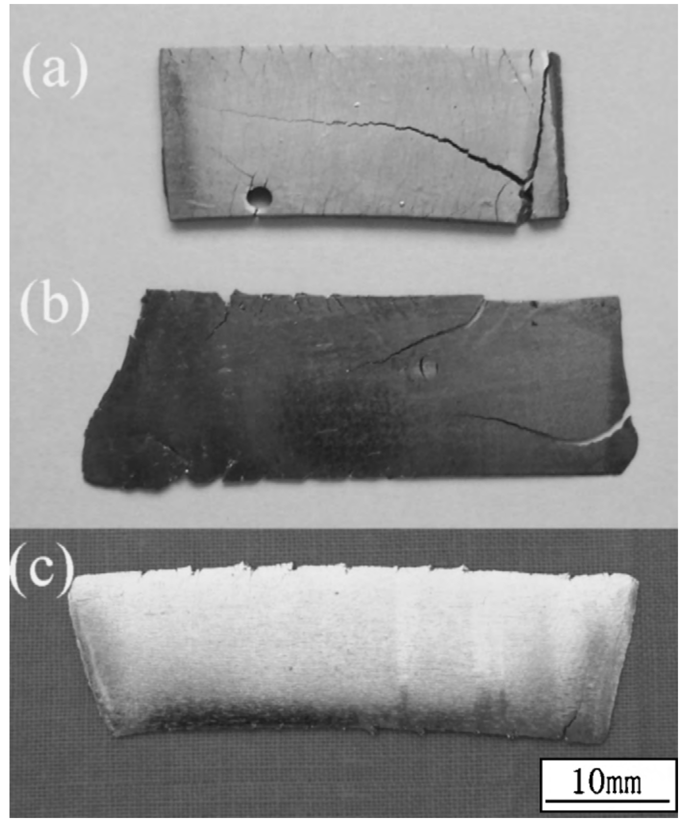

Fig. 4. Suction cast sheet of Fe–6.5 wt.% Si alloy after cold rolling at reduction of: (a) 25%, (b) 35% and (c) 44%.

The cold workability of rapidly quenched Fe–6.5 wt.% Si sheets with the same solidification rate was also dependent on the reduction per pass. The suction cast sheet was cold rolled with different reduction. There were many cracks for the suction cast sheet with reduction of 25% and 35% as shown in Fig. 4(a) and (b). The sample with reduction of 44% in Fig. 4(c) exhibited a uniform deformation and only some side cracks.

The workability variation with the reduction per pass results from the plastic deformation heat and friction heat during cold rolling. Higher rolling reduction leads to higher strain rate and higher flow stress. Therefore, a more significant temperature rise occurs during cold rolling with higher reduction [22]. The temperature rise of Fe–6.5 wt.% Si alloy sheet was calculated using the closed form formula suggested by Roberts [23]

$$\Delta T = \frac{1-(r/4)}{1-(r/2)} \cdot \frac{\sigma_p \ln(1/(1-r))}{\rho c_p} \tag{3}$$

in which ΔT is the temperature rise, r is the reduction per pass, σ_p is the flow strength, ρ is the density, and c_p is the specific heat. The results are shown in Table 3, where S1–S3 designate samples in Fig. 4(a–c), respectively.

Table 3
Temperature rise during cold rolling for suction cast samples.

Sample	Reduction (%)	Strain rate (s^{-1})	Stress (MPa)	ΔT (°C)
S1	25	3.4	1600	115
S2	35	5.9	1700	190
S3	44	6.8	1800	281

Shin et al. investigated the elongation of hot-rolled Fe–6 wt.% Si specimens at different temperatures, and revealed that the sheet exhibited almost zero elongation at room temperature and above 10% at 150 °C [4]. One can observe that ductility of this alloy is very sensitive to the temperature and much improved above 150 °C. According to Table 3, the temperature rise was 281 °C during rolling with a reduction of 44%. The temperature was high enough to improve the ductility of the sheet. Considering the small size of the samples, large amount of the heat would transfer to the rolls and the temperature rise would not be as high as calculated by Eq. (3). That is the reason why a reduction of 35% was not enough to improve ductility for cold rolling. One can conclude that high reduction would bring advantageous for cold rolling. After cold rolling, the degree of order was decreased. The sheet would be ductilized to be cold rolled. The combination of rapid quenching and high reduction of cold rolling provides an effective way to produce cold rolled sheet of Fe–6.5 wt.% Si alloy.

4. Conclusions

(1). Rapid quenching is useful to decrease the grain size and micro-hardness compared with conventionally cast method for Fe–6.5 wt.% Si alloy. The anti-Hall–Petch effect lies on the removal of $D0_3$ phases.

(2). High reduction brings advantageous for cold rolling due to temperature rise. Rapid quenching combined with high reduction provides an effective way to produce cold rolled Fe–6.5 wt.% Si alloy sheet.

Acknowledgements

Financial support from the Major State Basic Research Development Program of China (973 Program, No. 2006CB605205-2), and the National Natural Science Foundation of China (General Program, No. 50771018) is gratefully acknowledged.

References

[1] R.M. Bozorth, Ferromagnetism, Van Nostrand, New York, 1951, p. 81.
[2] E. Rabkin, B. Straumal, V. Semenov, W. Gust, B. Predel, Acta Metall. Mater. 43 (1995) 3075–3083.
[3] K. Raviprasad, K. Chattopadhyay, Acta Metall. Mater. 41 (1993) 609–624.
[4] J.S. Shin, Z.H. Lee, T.D. Lee, E.J. Lavernia, Scripta Mater. 45 (2001) 725–731.
[5] Y. Takada, M. Abe, S. Masuda, J. Inagaki, J. Appl. Phys. 64 (1988) 5367–5369.
[6] M.C.A. Silva, C. Bolfarini, C.S. Kiminami, Mater. Sci. Forum 498–499 (2005) 111–118.
[7] R. Li, Q. Shen, L.M. Zhang, T. Zhang, J. Magn. Magn. Mater. 281 (2004) 135–139.
[8] T. Ros-Yanez, Y. Houbaert, V.G. Rodriguez, J. Appl. Phys. 91 (2002) 7857–7859.
[9] H. Seifert, M. Jurisch, J. Tobisch, C.G. Oertel, Mater. Sci. Eng. A 133 (1991) 292–296.
[10] K.I. Arai, N. Tsuya, K. Ohmori, IEEE Trans. Magn. 17 (1981) 3154–3156.
[11] T. Watanabe, H. Fujii, H. Oikawa, K.I. Arai, Acta Metall. 37 (1989) 941–952.
[12] H. Nakamura, N. Tsuya, Y. Saito, Y. Katsumata, Y. Harada, J. Appl. Phys. 64 (1988) 5682–5683.
[13] Y. Ono, T. Ichiryu, I. Ohnaka, I. Yamauchi, J. Alloys Compd. 289 (1999) 277–284.
[14] K.N. Kim, L.M. Pan, J.P. Lin, Y.L. Wang, Z. Lin, G.L. Chen, J. Magn. Magn. Mater. 277 (2004) 331–336.
[15] J.S. Shin, J.S. Bae, H.J. Kim, H.M. Lee, T.D. Lee, E.J. Lavernia, Z.H. Lee, Mater. Sci. Eng. A 407 (2005) 282–290.
[16] R.W. Cahn, Physical Metallurgy Part II, Elsevier Science, Amsterdam, 1983, p. 1246.
[17] J.E. Wittig, G. Frommeyer, Metall. Mater. Trans. A 39A (2008) 252–265.
[18] J.S. Shin, S.M. Lee, B.M. Moon, H.M. Lee, T.D. Lee, Z.H. Lee, Met. Mater. Int. 10 (2004) 581–587.
[19] H. Bakker, G.F. Zhou, H. Yang, Prog. Mater. Sci. 39 (1995) 159–241.
[20] J.S.C. Jang, C.C. Koch, J. Mater. Res. 5 (1990) 498–510.
[21] M.M. Dadras, D.G. Morris, Scripta Metall. Mater. 28 (1993) 1245–1250.
[22] Z.C. Lin, C.C. Shen, J. Mater. Process. Technol. 110 (2001) 10–18.
[23] W.L. Roberts, Cold Rolling of Steel, Marcel Dekker, Inc., New York, 1978, pp. 332–397.